

DRAFT VERSION MARCH 11, 2019

Typeset using **LATEX** **preprint** style in AASTeX62

Proton-proton collisions in the turbulent solar wind: Hybrid Boltzmann-Maxwell simulations

O. PEZZI,^{1,2} D. PERRONE,³ S. SERVIDIO,⁴ F. VALENTINI,⁴ L. SORRISO-VALVO,^{5,6} AND P. VELTRI⁴

¹*Gran Sasso Science Institute, Viale F. Crispi 7, I-67100 L'Aquila, Italy*

²*INFN/Laboratori Nazionali del Gran Sasso, Via G. Acitelli 22, I-67100 Assergi (AQ), Italy*

³*Department of Physics, Imperial College London, London SW7 2AZ, United Kingdom*

⁴*Dipartimento di Fisica, Università della Calabria, I-87036 Cosenza, Italy*

⁵*Nanotec-CNR, Sede di Rende, I-87036 Rende, Italy*

⁶*Departamento de Física, Escuela Politécnica Nacional, Quito, Ecuador*

(Dated: March 11, 2019)

ABSTRACT

The mechanism of heating for hot, dilute and turbulent plasmas represents a long-standing problem in space physics, whose implications concern both near-Earth environments and astrophysical systems. Here, in order to explore the possible role of inter-particle collisions, for the first time, collisional and collisionless simulations of plasma turbulence have been compared using Eulerian Hybrid Boltzmann-Maxwell simulations, that explicitly model the proton-proton collisions through the nonlinear Dougherty operator. Although collisions do not significantly influence the statistical characteristics of the turbulence, they strongly suppress the production of non-thermal features in the proton distribution function. The latter consists in a suppression of the enstrophy/entropy cascade in the velocity space, damping the spectral transfer towards large Hermite modes. Moreover, we observe that dissipation is located within regions of strong current activity, confirming that the heating process in turbulent plasmas is spatially inhomogeneous.

1. INTRODUCTION

Understanding the dynamics of turbulent and weakly-collisional plasmas represents a challenging problem, whose implications affect a rich variety of systems, ranging from astrophysical environments, e.g. supernovae remnants, inter-galactic medium and astrophysical jets (Parizot et al. 2006; Webb et al. 2018), to near-Earth environments such as the solar wind and the planetary magnetospheres (Zimbardo et al. 2010; Bruno & Carbone 2013; Chen 2016). In these systems, the energy injected at large scales as gradients is transferred to increasingly larger wave-vectors, producing smaller scale fluctuations – as in typical turbulence processes. Plasma vortices and magnetic coherent structures are routinely recovered in space and astrophysical plasma measurements (Servidio et al. 2012; Greco et al. 2012; Perrone et al. 2016; Greco et al. 2016; Perrone et al. 2017; Wang et al. 2019) and observations support the standard picture of intermittent, inhomogeneous features of the tur-

Corresponding author: Oreste Pezzi

oreste.pezzi@gssi.it

bulent cascade (Sorriso-Valvo et al. 1999; Veltri 1999; Alexandrova et al. 2008; Sahraoui et al. 2007; Perri et al. 2012; Karimabadi et al. 2013a; Bruno & Telloni 2015; Carbone et al. 2018).

When the turbulent cascade reaches these small spatial and temporal scales, the energy associated with fields fluctuations can be transferred to the particle velocity distribution function (VDF) (Servidio et al. 2015), where it is eventually dissipated (Vaivads et al. 2016). Significant efforts have been devoted to understand plasma dynamics at such scales and different dissipation mechanisms have been invoked (Sorriso-Valvo et al. 2007; Marino et al. 2008; Chandran 2010; Osman et al. 2011, 2012; Wu et al. 2013; Vech, Klein & Kasper 2017; Yang et al. 2017; Shay et al. 2018; Dae Yoon & Bellan 2018; Chasapis et al. 2018; Sorriso-Valvo et al. 2019). However, several of the proposed heating mechanisms explicitly neglect the role of inter-particle collisions.

Even if the common thought is that collisions act, on average, at large characteristic time and space scales (Spitzer 1956; Hernandez & Marsch 1985; Kasper, Lazarus & Gary 2008; Maruca et al. 2014; Tracy et al. 2016; Chhiber et al. 2016; Vafin, Riazantseva & Pohl 2019), they may also be non-negligible at small scales, especially when plasma turbulence develops strong gradients in the velocity space. These features are routinely observed in the solar wind and the magnetosheath, manifesting as strong temperature anisotropy enhancements, beams of accelerated particles, rings, and velocity-space vortices (Marsch 2006; Servidio et al. 2015; Wilder et al. 2016; Lapenta et al. 2017). Because of these observational evidences, a turbulent velocity-space entropy cascade has been conjectured (Schekochihin et al. 2016) and it has been recently observed in the Earth's magnetosheath (Servidio et al. 2017) and in Eulerian hybrid Vlasov simulations (Cerri, Kunz & Califano 2018; Pezzi et al. 2018a).

Recently, the role of collisions has been considered with novel attention (Tatsuno et al. 2009; TenBarge & Howes 2013; Escande, Elskens & Doveil 2015; Tigik et al. 2016; Banón Navarro et al. 2016; Pezzi, Valentini & Veltri 2016; Pezzi 2017). The reason for this renewed interest is, at least, two-fold. First, collisions are the mechanism which operates the transition from collisionless (Vlasov) to collisional dynamics, since the collisional operators often satisfy the Boltzmann H-theorem for the entropy growth. This aspect is crucial for investigating the small-scale end of the turbulent cascade, where the physical information contained into phase-space structures needs to be degraded by means of irreversible processes. To properly describe the plasma heating from a well-posed thermodynamics viewpoint, the introduction of an irreversible mechanism, such as collisions, is then crucial. Second, it has been recently proposed that plasma collisionality may be enhanced by the presence of fine velocity-space structures (Pezzi, Valentini & Veltri 2016; Pezzi 2017). Indeed, small-scale velocity-space structures are rapidly smoothed out by collisions, suggesting a local enhancement of collisionality. In other words, the presence of fine phase-space perturbations, incessantly produced by plasma turbulence at kinetic scales, makes collisions act on characteristic times that are much smaller than predicted upon a quasi-Maxwellian assumption (Pezzi, Valentini & Veltri 2016; Pezzi 2017). This paves the way to a novel scenario, where the production of finer velocity space structures occurs, until the characteristic time associated with their development is balanced by the characteristic time associated with the dissipation of such structures. A similar behavior has been very recently found in solar-wind data for bi-Maxwellian VDFs (Vafin, Riazantseva & Pohl 2019). This type of dissipation would act as a purely thermodynamic heating, since the free energy contained into the velocity space structures –which could be converted into other forms of ordered energy by means of several collisionless mechanisms, e.g. micro-instabilities (Gary 2005; Matteini et al. 2012;

Chen et al. 2016; Hellinger et al. 2017)– is actually destroyed by an irreversible process. The complete description of such scenario is probably beyond the capability of any present *in-situ* observations (Pezzi et al. 2018b), hence addressing it via numerical simulations is of fundamental importance.

Pezzi, Valentini & Veltri (2016) have described the collisionality enhancement by modeling collisions through the fully nonlinear Landau operator (Landau 1936; Rosenbluth, MacDonald & Judd 1957) and focusing on a force-free, homogeneous plasma. The latter assumption represents a caveat that allows to model collisions with a “proper” operator, such as the fully nonlinear Landau operator (that can be derived from first-principles, and holds an H-theorem for the entropy growth). However, the computational cost of the Landau operator is nowadays too demanding for performing self-consistent simulations [see Pezzi (2017) for further details]. Besides, the choice of the more general Lenard-Balescu operator (Lenard 1960; Balescu 1960) –which, unlike the Landau operator, takes also into account the presence of spatial fluctuations through the dispersion function– would make any computational approach unaffordable.

In the present work, we get rid of the approximation of force-free, homogeneous plasma by performing *ab-initio* collisional, self-consistent, Eulerian Hybrid Boltzmann-Maxwell simulations of a turbulent plasma. This framework has been widely adopted for describing plasma turbulence at proton and sub-proton scales, using the collisionless Vlasov counterpart (Servidio et al. 2015; Valentini et al. 2016; Cerri, Servidio & Califano 2017; Groselj et al. 2017; Pezzi et al. 2018a; Perrone et al. 2018). In order to make self-consistent simulations affordable, it is necessary to reduce the complexity of the collisional operator. To this aim, we model collisions through the nonlinear Dougherty operator (Dougherty 1964; Dougherty & Watson 1967; Dougherty, Watson & Hellberg 1967). This is an *ad-hoc* collisional operator, already adopted in self-consistent Vlasov-Poisson simulations to describe the collisional dissipation of nonlinear electrostatic waves (Pezzi, Valentini & Veltri 2015b) and to model inter-particle collisions in non-neutral plasma columns (Anderson & O’Neil 2007a,b). It has been also compared to the Landau operator both by means of Eulerian numerical simulations concerning the relaxation of out-of-equilibrium distribution functions in a homogeneous force-free plasma (Pezzi, Valentini & Veltri 2015a), and in the Fourier-Hermite space (Pezzi et al. 2018b).

In this paper, we compare the collisional (Boltzmann) and the collisionless (Vlasov) model of plasma turbulence by means of direct numerical simulations. In particular, starting with the same initial conditions, we analyze Hybrid Boltzmann-Maxwell (HBM) and Hybrid Vlasov-Maxwell (HVM) simulations, investigating whether collisions affect the general properties of turbulence and the generation of non-thermal features in the proton VDF. Moreover, we study the correlation between the plasma collisionality, evaluated through the collisional dissipation rate (Banón Navarro et al. 2016), and the presence of strong coherent structures. We also discuss the implication of taking into account inter-particle collisions in terms of collisional age (Hernandez & Marsch 1985; Kasper, Lazarus & Gary 2008; Maruca, Kasper & Bale 2011) and entropy density (Parks et al. 2012; Gary et al. 2018). Finally, we focus on the effect of collisions on the velocity-space cascade (Servidio et al. 2017; Cerri, Kunz & Califano 2018; Pezzi et al. 2018a).

2. NUMERICAL MODEL

The numerical model employed for this study is based on the HVM system of equations (Valentini et al. 2007). Here we extend the HVM model by retaining the effect of proton-proton

collisions. Dimensionless HBM equations, in presence of collisions, are:

$$\frac{\partial f}{\partial t} + \mathbf{v} \cdot \frac{\partial f}{\partial \mathbf{x}} + (\mathbf{E} + \mathbf{v} \times \mathbf{B}) \cdot \frac{\partial f}{\partial \mathbf{v}} = C(f, f) \quad (1)$$

$$\frac{\partial \mathbf{B}}{\partial t} = -\nabla \times \mathbf{E} = \nabla \times \left[\mathbf{u} \times \mathbf{B} - \frac{\mathbf{j} \times \mathbf{B}}{n} + \frac{\nabla P_e}{n} - \eta \mathbf{j} \right] \quad (2)$$

where $f(\mathbf{x}, \mathbf{v}, t)$ is the proton VDF, \mathbf{E} and \mathbf{B} are the electric and magnetic field, respectively, and $C(f, f)$ is the collisional operator. The current density is $\mathbf{j} = \nabla \times \mathbf{B}$, the proton density n and bulk velocity \mathbf{u} are computed as the first two moments of f , while P_e is the isothermal pressure of the massless fluid electrons; quasi-neutrality is also assumed. Time, velocities and lengths are respectively scaled to the inverse proton cyclotron frequency $\Omega_{cp}^{-1} = m_p c / e B_0$, to the Alfvén speed $c_A = B_0 / \sqrt{4\pi n_0 m_p}$, and to the proton skin depth $d_p = c_A / \Omega_{cp}$, m_p , e , c , B_0 and n_0 being the proton mass, the unit charge, the light speed, the background magnetic field and the equilibrium proton density. Electron inertia effects have been neglected in the Ohm's law, while a small resistivity ($\eta = 10^{-3}$) is accurately introduced to suppress numerical instabilities.

Collisions are modeled through the nonlinear Dougherty operator (Dougherty 1964; Dougherty & Watson 1967; Dougherty, Watson & Hellberg 1967):

$$C(f, f) = \nu \frac{n}{T^{3/2}} \frac{\partial}{\partial v_j} \left[T \frac{\partial f}{\partial v_j} + (v - u)_j f \right], \quad (3)$$

where ν is the normalized collisional frequency:

$$\nu = \frac{g \ln \Lambda \beta_p^{3/2}}{16\pi \sqrt{2} \xi} \quad (4)$$

$\xi = c_A/c$, $\beta_p = 2v_{th,p}^2/c_A^2$ ($v_{th,p} = \sqrt{k_B T_{0,p}/m_p}$, the proton thermal speed) and $\ln \Lambda$ and g are the Coulombian logarithm and the plasma parameter, respectively. The collisional frequency, ν , is a numerical parameter which evaluates the strength of the collisional operator with respect to the other terms in the Vlasov equation. By considering the typical solar-wind parameters in Eq. (4), one gets $\nu \sim 10^{-5}$. To appreciate the role of collisions without irremediably increasing their computational cost, we used a collisional frequency ν which is two orders of magnitude larger than in typical solar-wind conditions. Note that the role of η and ν is physically different. In particular, ν is related to proton-proton collisions while η can be related to electron-proton collisions (Spitzer 1956), that are not explicitly considered in the present work.

Equations (1)–(2) have been integrated in a 2.5D-3V phase space domain (the three-dimensional velocity space is fully described while, in the physical space, the three vector components depend only on x and y). Despite the dimensionality approximation, the 2.5D physical space is still able to capture the features of several physical processes (Karimabadi et al. 2013; Wan et al. 2015; Servidio et al. 2015; Li et al. 2016; Pezzi et al. 2017a,b; Franci et al. 2018). The size of the double-periodic spatial domain is $L_x = L_y = L = 2\pi \times 20d_p$ and it is discretized with 512 grid-points in each direction, while the velocity domain is discretized with 71 grid-points in the range $v_j = [-5v_{th,p}, 5v_{th,p}]$ ($j = x, y, z$) with the boundary condition $f(v_j > 5v_{th,p}) = 0$. A detailed description of the HVM algorithm can be found in Valentini et al. (2007) and Vásconez et al. (2015). The basic current-advance-method

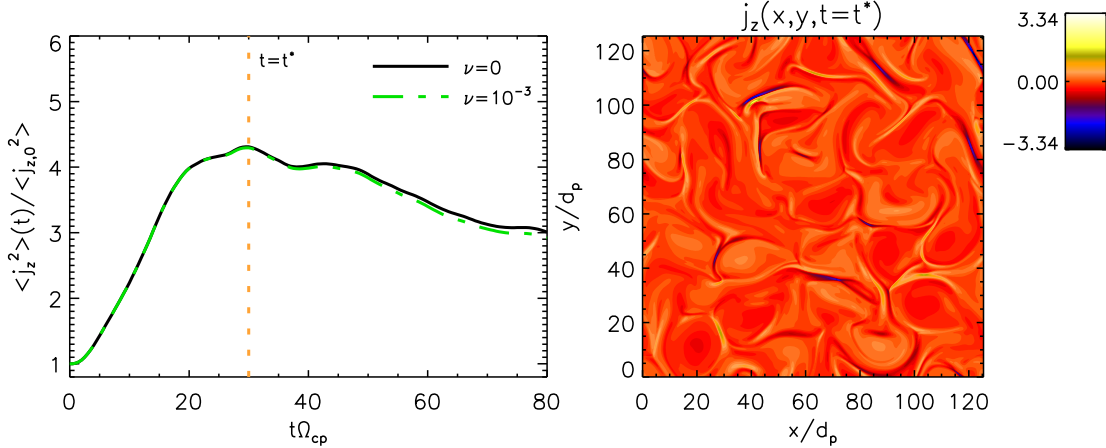


Figure 1. (Color online) Left: Temporal evolution of $\langle j_z^2 \rangle(t)$ for the Vlasov (black solid line) and Boltzmann (green dash-dotted line) runs. The vertical orange dashed line indicates the peak of the turbulent activity ($t^* = 30\Omega_{cp}^{-1}$). Right: Contour plot of $j_z(x, y)$ for the collisional case at $t = t^*$. The same pattern is found in the collisionless case.

algorithm, implemented in the collisionless version of the code, is here modified by introducing the collisional step (Filbet & Pareschi 2002; Pezzi et al. 2013).

The initial equilibrium is composed of a homogeneous, Maxwellian proton VDF, embedded in an uniform out-of-plane magnetic field $\mathbf{B}_0 = B_0 \mathbf{e}_z$ ($B_0 = 1$) and $\beta_p = 2$. The equilibrium is then initially perturbed by imposing large-amplitude magnetic field $\delta\mathbf{b}$ and bulk velocity $\delta\mathbf{u}$ perturbations. The energy is injected in the wave-number range $k \in [0.1, 0.3]$, being $k = mk_0$ with $2 \leq m \leq 6$ and $k_0 = 2\pi/L$, in such a way that the spectrum is initially flat; phases are random. The r.m.s. level of fluctuations is $\delta b/B_0 = 1/2$. No density perturbations nor parallel perturbations are introduced at $t = 0$. Two different runs have been performed, that differ only by the presence of the collisional operator, while the equilibrium background and the perturbations amplitude are the same. In particular, the first run is collisionless (Vlasov), namely $\nu = 0$; while the second run is weakly collisional (Boltzmann), with $\nu = 10^{-3}$. We follow the evolution of the system up to $t_{fin} = 80\Omega_{cp}^{-1}$. The computational cost of the two simulations is quite large, consisting of ~ 1 million CPU-hours on the supercomputer MARCONI at CINECA, with a massively parallelized and optimized code.

3. EFFECTS OF COLLISIONS ON TURBULENCE

At the beginning of the simulations, initial perturbations nonlinearly couple and produce a cascade towards smaller scales. The generation of small-scale fluctuations can be appreciated in the temporal evolution of $\langle j_z^2 \rangle$ shown in left panel of Fig. 1, where $\langle \dots \rangle$ denotes the average on the spatial domain. We observe that $\langle j_z^2 \rangle$ initially increases, then saturates at an almost constant value, in the temporal range $t \in [20, 40]\Omega_{cp}^{-1}$, and finally decreases for the presence of numerical dissipation induced by the finite mesh-size of the numerical grid and the small value of the numerical resistivity (Valentini et al. 2014). The peak of the turbulent activity, indicated with a vertical orange dashed line, occurs at $t^*\Omega_{cp} = 30$. Proton collisions do not seem to have a noticeable effect in the evolution of the current density. Indeed, the temporal evolution of $\langle j_z^2 \rangle$ is comparable in the Vlasov (black solid line) and Boltzmann (green dash-dotted line) cases.

The right panel of Fig. 1 shows the contour plot of the out-of-plane current density, $j_z(x, y)$, at $t = t^*$ for the collisional case. This quantity, related to the in-plane magnetic field gradients (the dominant component in our simulation), exhibits a turbulent and intermittent pattern, characterized by the presence of vortices, magnetic islands, current sheets and X-points, suggesting also the presence of magnetic reconnection. A similar behavior is observed for $j_z(x, y)$ in the collisionless case (not shown here).

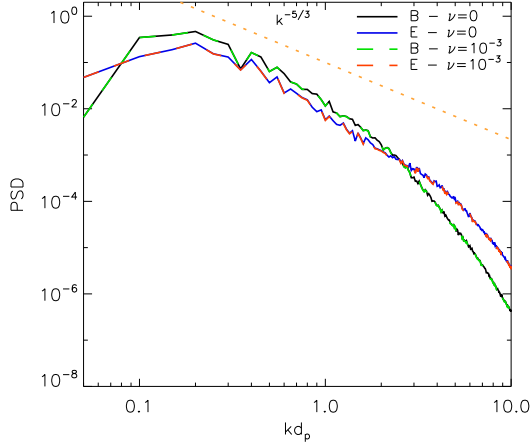


Figure 2. (Color online) Omni-directional PSDs of the magnetic field for the collisionless (black solid) and collisional (green dashed) cases; and of the electric field for the collisionless (blue solid) and collisional (red dashed) cases. The orange dashed line indicates the Kolmogorov expectation.

In order to inspect the turbulence evolution at proton and sub-proton scales, we computed at $t = t^*$ the omni-directional (perpendicular) power spectral densities (PSDs) for both magnetic and electric fields, as a function of kd_p . Fig. 2 shows the PSDs for the collisionless (solid line) and collisional (dashed line) runs. The electric and magnetic spectra obtained in the two runs perfectly match, and reveal the typical features observed in solar-wind plasma. Indeed, similarly to previous numerical experiments (Perrone et al. 2013; Valentini et al. 2016; Pezzi et al. 2018a), an inertial-like range is observed, where the magnetic PSD recalls the Kolmogorov prediction (orange dashed-line) (Kolmogorov 1941). Around $kd_p \sim 1$, the usual spectral steepening is recovered (Leamon et al. 1998). At sub-proton scales, the electric activity becomes dominant (Bale et al. 2005), while density fluctuations are always very low (not shown).

4. EFFECTS OF COLLISIONS ON KINETIC PHYSICS

Although collisions do not play a significant role in modifying the statistical characteristics of turbulence, they strongly change the production and the evolution of kinetic (non-thermal) features. The temporal evolution of the entropy (not shown here) indicates that the entropy growth is much larger in the collisional case than in the collisionless one (where entropy slightly increases for grid effects). The proton temperature (averaged on the spatial domain) grows similarly for the two cases. Indeed –in the hybrid case and only including proton-proton collisions– the Dougherty operator, as the Landau one, does not affect the evolution of the second order moment of the distribution function. Note that, by considering the electron dynamics and electron-electron and ion-electron collisions, the scenario may be different, since energy transfer between species is allowed.

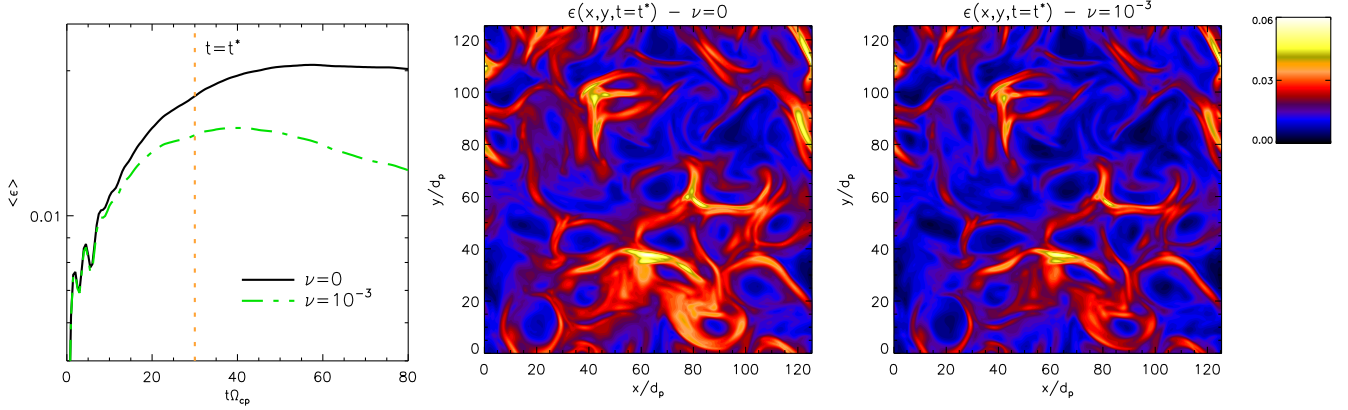


Figure 3. (Color online) Left: Temporal evolution of $\langle \epsilon \rangle(t)$ for the collisionless (black solid) and weakly-collisional (green dash-dotted) runs. The orange dashed vertical line indicates $t = t^* = 30\Omega_{cp}^{-1}$. Middle: Contour plot of $\epsilon(x, y)$ at $t = t^*$ for the Vlasov run. Right: Contour plot of $\epsilon(x, y)$ for the Boltzmann simulation.

In order to quantitatively evaluate the out-of-equilibrium kinetic features in the proton VDF, we make use of the parameter ϵ , defined as follows (Greco et al. 2012; Valentini et al. 2016; Pezzi et al. 2017a):

$$\epsilon(\mathbf{x}, t) = \frac{1}{n(\mathbf{x}, t)} \sqrt{\int [f(\mathbf{x}, \mathbf{v}, t) - g(\mathbf{x}, \mathbf{v}, t)]^2 d^3v}, \quad (5)$$

where $g(\mathbf{x}, \mathbf{v}, t)$ is the Maxwellian distribution function associated to the observed $f(\mathbf{x}, \mathbf{v}, t)$, i.e. with the same density, bulk speed and temperature. The left panel of Figure 3 reports the temporal evolution of $\langle \epsilon \rangle(t)$. In the collisionless case, $\langle \epsilon \rangle(t)$ increases during the set-up of the nonlinear cascade and then saturates at a nearly constant value. On the other hand, when collisions are in place, $\langle \epsilon \rangle(t)$ slowly decreases after the peak of the turbulent activity (orange dashed line). This global behavior, similar to the enstrophy in fluid flows, suggests that the velocity-space complexity saturates in the ideal (Vlasov) case, while in the Boltzmann plasma there is the tendency to return to Maxwellianity, i.e. $\epsilon \rightarrow 0$. This is consistent with the pattern observed in the contour plots of $\epsilon(x, y, t = t^*)$, where we find a more complex structure in the case without collisions (middle panel), with intense and broad regions of non-Maxwellianity, with respect to the collisional run (right panel). In the latter case, these structures are weaker and narrower. However, in both cases, non-Maxwellian regions are located close to turbulent current sheets.

The time evolution of $\epsilon(x, y)$ in the two runs shows substantial differences, as seen by comparing Fig. 3 with the top panels of Fig. 4, where maps of $\epsilon(x, y)$ at the final time of each run are shown. It is evident that collisions strongly reduce $\epsilon(x, y)$ with time in the whole volume, effectively leading the plasma towards the thermal equilibrium, except for small regions near the turbulent current structures. On the other hand, in the collisionless case, the areas with large $\epsilon(x, y)$ slightly spread around the current sheets, thus increasing the proton global deviation from Maxwellian with time. Additionally, the amplitude of the most intense values weakly decreases with time. This is probably due to collisionless processes, such as kinetic instabilities, that drive back the free energy contained in non-equilibrium features of the proton VDF into the electromagnetic fields (Hellinger et al. 2017).

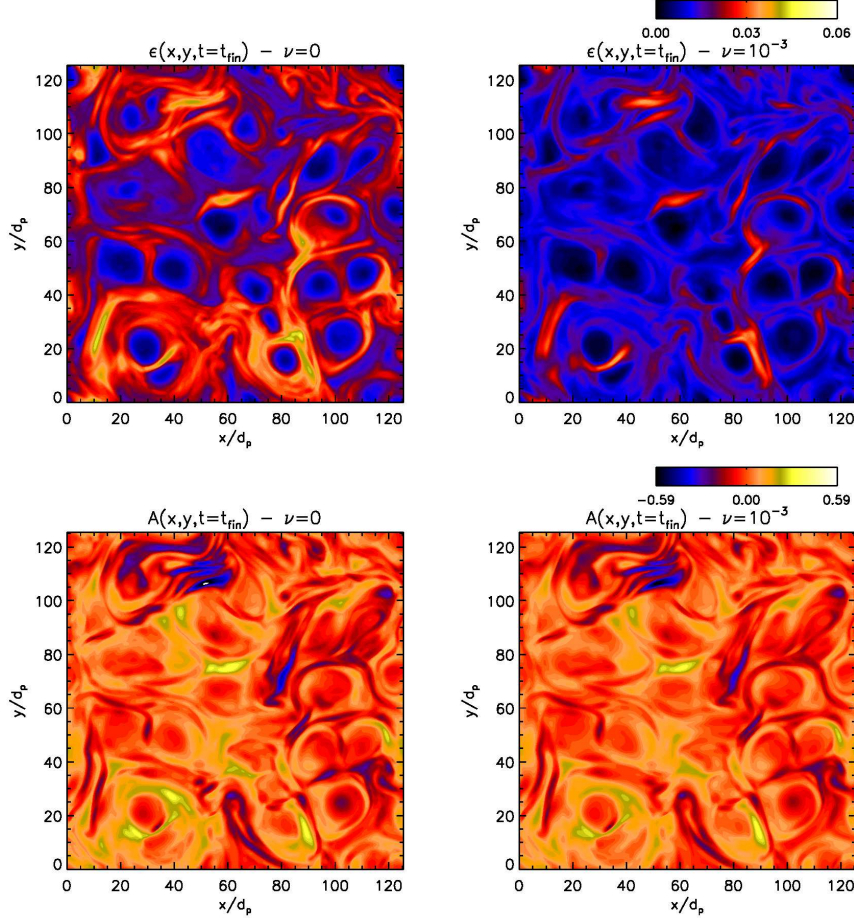


Figure 4. (Color online) Contour plots of $\epsilon(x, y)$ (top) and $A(x, y)$ (bottom) at $t = t_{fin} = 80\Omega_{cp}^{-1}$ for the Vlasov (left) and Boltzmann (right) cases.

Bottom panels of Fig. 4 show the proton temperature anisotropy $A = 1 - T_{\perp}/T_{\parallel}$, evaluated with respect to the background magnetic field, at the end of each run. No significant differences are found in the two simulations, suggesting that collisions contribute to dissipate purely kinetic characteristics (i.e. which cannot be interpreted in terms of anisotropic pressure tensor models (Chew, Goldberger & Low 1956)) much faster than temperature anisotropies. This result may be also interpreted as an evidence that collisions smooth fine velocity space structures on different characteristic times, which depend on the considered velocity scales, as suggested by Pezzi, Valentini & Veltri (2016) and Pezzi (2017).

5. COLLISIONAL DISSIPATION RATES AND ENTROPY DENSITY

Understanding whether or not collisions can compete with other processes, by estimating the characteristic time on which they play an efficient role, is decisive. Collisional characteristic times depend on the strength of velocity space gradients, so that collisional temporal scales may have a local dependence on velocity coordinates (Pezzi, Valentini & Veltri 2016). To this aim, a modeling effort to estimate the importance of collisions, by also retaining the description of fine velocity structures formation, is fundamental. In this perspective, Banón Navarro et al. (2016) derived a collisional dissipation rate, that is local in physical space and integrated in velocity space. We would like to stress

that the word dissipation is meant as irreversible enstrophy/entropy dissipation, and is not related to energy, which is conserved in this model of collisions. Although the definition in [Banón Navarro et al. \(2016\)](#) lacks in the inclusion of the possible dependence of collisional times on velocity coordinates, it is extremely useful to figure out if collisional rates are correlated with other important physical phenomena, such as the presence of current sheets and magnetic reconnection. Additionally, it could be easily applied to *in-situ* observations of space plasmas.

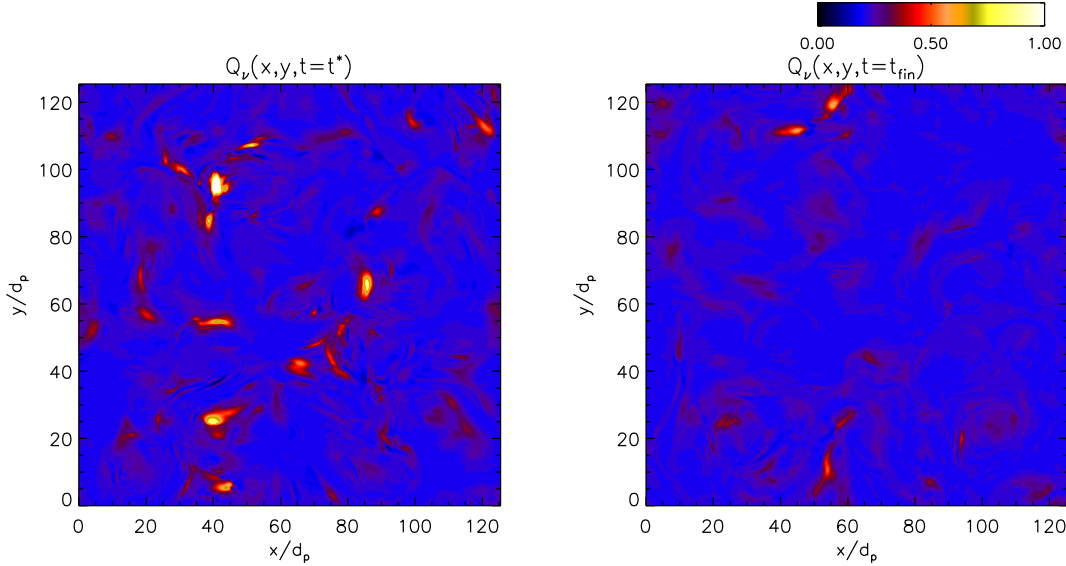


Figure 5. (Color online) Contour plots of $Q_\nu(\mathbf{x}, t)$ for the Boltzmann simulation at $t = t^* = 30\Omega_{cp}^{-1}$ (left) and $t = t_{fin} = 80\Omega_{cp}^{-1}$ (right). In each panel the color scale is the same and, for the sake of simplicity, quantities have been normalized to $Q_{\nu,max} = 4.3 \times 10^{-6}$, which is the maximum of each shown quantity.

Here we adopt the following definition of the collisional dissipation rate, which is similar to the one defined by [Banón Navarro et al. \(2016\)](#):

$$Q_\nu(\mathbf{x}, t) = \frac{1}{n_0} \int d^3v \, C(f, f) . \quad (6)$$

Q_ν represents a proxy of the collisional operator strength in a local spatial point and at a given instant of time: i.e., given the distribution function and its moments, one computes the collisional operator and extrapolates Q_ν , which gives insight about the collision efficiency in the *future* evolution of the system. Note that the above definition differs from the collisional age ([Livi, Marsch & Rosenbauer 1986](#); [Kasper, Lazarus & Gary 2008](#); [Maruca, Kasper & Bale 2011](#); [Maruca et al. 2014](#); [Chhiber et al. 2016](#)), which is a proxy of the number of collisions occurring in a solar wind parcel traveling in the interplanetary medium (without retaining the effect of fine velocity structures), i.e. related to the *past* evolution of the plasma.

Figure 5 shows the contour plots of $Q_\nu(x, y)$ at $t = t^*$ (left) and $t = t_{fin}$ (right) for the collisional simulation. At $t = t^*$, Q_ν is qualitatively correlated with the contours of j_z shown in Fig. 1; while Q_ν is vanishing nearly everywhere at the end of the simulation. This confirms that collisions slowly but incessantly contribute to the dissipation since the beginning of the simulation, leading the plasma towards the thermal equilibrium –as also suggested by the contour plots of ϵ in Fig. 3 and 4. This

resembles the role of dissipative terms like $\nabla^2 \mathbf{u}$ in Euler simulations, that in fact irreversibly dissipate the turbulent energy. On the other hand, the collisional dissipation rates remain almost unchanged during the temporal evolution in the collisionless case (not shown here), since there are no physical processes able to dissipate entropy fluctuations.

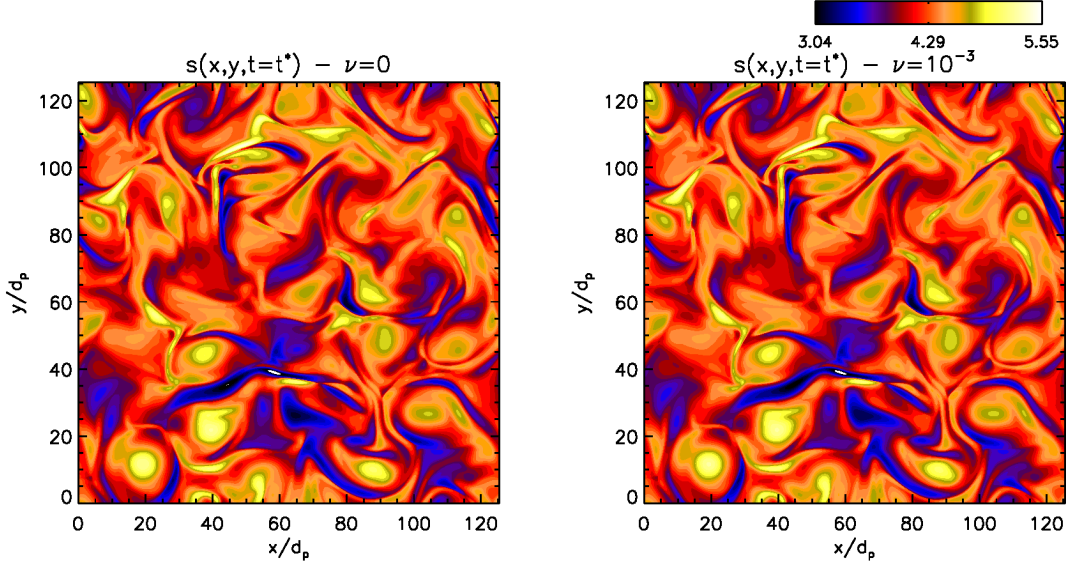


Figure 6. (Color online) Contour plots of $s(\mathbf{x}, t)$ for both collisionless (left) and weakly-collisional (right) runs at $t = t^* = 30\Omega_{cp}^{-1}$.

We conclude this section by finally focusing on the entropy density, defined as:

$$s(\mathbf{x}, t) = - \int d^3v f \log f . \quad (7)$$

This quantity has been widely adopted for describing “entropy production” in shock waves (Parks et al. 2012) and in collisionless plasma turbulence simulations (Gary et al. 2018). The physical meaning of s is not related to the Boltzmann thermodynamic entropy S . Indeed, while the former is local in physical space, the latter includes global integration over the whole phase space. Furthermore, only the Boltzmann entropy S satisfies the H-theorem. Note also that, for small perturbations of the VDF, i.e. $\delta f = f - f_0$, the variation of s can be expressed as:

$$\Delta s = s(\mathbf{x}, t) - s(\mathbf{x}, 0) \simeq - \int d^3v \left[\delta f (1 + \log f_0) + \frac{\delta f^2}{f_0} \right] \quad (8)$$

that is similar to ϵ (i.e. $\epsilon^2 n^2 \simeq \int d^3v \delta f^2$). Both quantities describe the presence of non-Maxwellian features in the proton VDF. In other words, the entropy density s is another proxy for highlighting the production of non-Maxwellian features.

Figure 6 displays the contour plot of $s(x, y)$ at $t = t^*$, for collisionless (left panel) and collisional (right panel) cases. No significant differences from both quantitative and qualitative perspective are found. Even at different time instants, slight differences between the HVM and HBM cases are recovered (not shown here). These small differences, which can be appreciated by averaging over

the spatial domain (i.e. by recovering the Boltzmann entropy definition), corresponds to the global entropy growth occurring in the collisional run. It is worth noting that the current definition of entropy density s may intrinsically hide differences during the temporal evolution of the system, since it also includes the adiabatic part. As recently proposed by Liang et al. (2019), the use of a velocity-space and physical-space entropy density may give insights on how dissipation actually occurs.

By comparing s (Fig. 6) and ϵ (Fig. 3), it is evident that the entropy density s also peaks at the center of vortices and magnetic islands, since significant contributions from the pressure terms are expected in these locations. On the other hand, ϵ peaks just close to strong current sheets (Servidio et al. 2012; Osman et al. 2011, 2012). Finally, in the Boltzmann case, ϵ decreases with time, while s does not show a significant temporal evolution (not shown). This probably indicates that ϵ , against s , is able to retain the effect of the collisional dissipation.

6. EFFECTS OF COLLISIONS ON THE PHASE-SPACE CASCADE

In this last section we investigate the development of a phase-space cascade, induced by the presence of turbulent fluctuations, as recently proposed in several works (Servidio et al. 2017; Cerri, Kunz & Califano 2018; Pezzi et al. 2018a; Eyink 2018; Schekochihin et al. 2016). The idea of this process is that turbulence in collisionless plasmas can initiate the production of a cascade-like process in the full phase-space, leading to the formation of non-Maxwellian features. Here, for the first time, we investigate this phase-space cascade in both Vlasov and Boltzmann simulations.

To analyze the phase-space details, we adopt a 3D Hermite transform representation of f , namely $f(\mathbf{v}) = \sum_{\mathbf{m}} f_{\mathbf{m}} \Psi_{\mathbf{m}}(\mathbf{v})$, where $\Psi_{\mathbf{m}}(\mathbf{v}) = \prod_j \psi_{m_j}(v_j)$ ($j = x, y, z$) and the 1D basis is:

$$\psi_m(v) = \frac{H_m\left(\frac{v-u}{v_{th}}\right)}{\sqrt{2^m m! \sqrt{\pi} v_{th}}} e^{-\frac{(v-u)^2}{2v_{th}^2}}. \quad (9)$$

In the above mother-function u and v_{th} are the local bulk and thermal speed, respectively, $m \geq 0$ is an integer (we simplified the notation suppressing the spatial dependence). The eigenfunctions obey the orthogonality condition $\int_{-\infty}^{\infty} \psi_m(v) \psi_l(v) dv = \delta_{ml}$. Since the basis is opportunely shifted in the local bulk speed frame and normalized to the local density and temperature, we focus on the presence of high-order fluctuations in the Hermite space. A Gaussian quadrature is also introduced to avoid spurious aliasing and convergence problems (Yin 2014; Servidio et al. 2017; Pezzi et al. 2018a). The accuracy of the Hermite transform is finally verified through the Parseval-Plancherel spectral theorem. The Hermite coefficients $f_{\mathbf{m}} = \int_{-\infty}^{\infty} f(\mathbf{v}) \Psi_{\mathbf{m}}(\mathbf{v}) d^3v$ have been computed for each spatial point. A highly deformed VDF generates plasma enstrophy, defined as

$$\Omega(\mathbf{x}) \equiv \int_{-\infty}^{\infty} \delta f^2(\mathbf{x}, \mathbf{v}) d^3v = \sum_{\mathbf{m} > 0} [f_{\mathbf{m}}(\mathbf{x})]^2. \quad (10)$$

Note that the enstrophy is related to the non-Maxwellian parameter, since $\Omega = \epsilon^2 n^2$, and is also intimately related to the entropy, when the level of fluctuations of the velocity distribution function is small.

In order to project the VDF over the Hermite basis, from a technical perspective, we set $N_m = 100$ modes in each velocity direction. To reduce the computational effort, the projection has been applied

to a subset of the original volume which represents a uniform coarse-graining of the original 512^2 spatial domain, whose size is 64^2 (the convergence of our decomposition is attained also for a coarser ensemble of 32^2 VDFs).

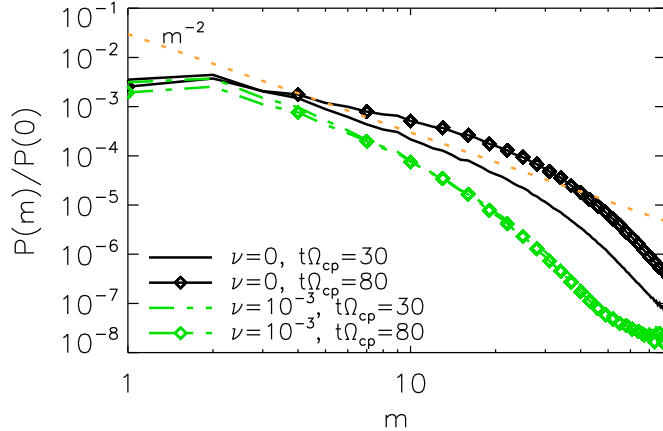


Figure 7. (Color online) Isotropic Hermite spectra $P(m)/P(0)$ for the collisionless case at $t = t^*$ (black solid) and $t = t_{fin}$ (black solid with diamonds) and for the collisional case at $t = t^*$ (green dash-dotted) and $t = t_{fin}$ (green dash-dotted with diamonds). The prediction for the magnetized case (m^{-2}) is reported in orange dashed line as a reference.

From the coefficients $f_{\mathbf{m}}(\mathbf{x}) \equiv f_{\mathbf{m}}(\mathbf{x}, \mathbf{m})$, we computed the enstrophy spectrum $P(m_x, m_y, m_z) = \langle f_{\mathbf{m}}(\mathbf{x})^2 \rangle$, where $\langle \dots \rangle$ indicates spatial average. The isotropic (omnidirectional) 1D Hermite spectrum is finally obtained by summing $P(m_x, m_y, m_z)$ over concentric shells of unit width, i. e. $P(m) = \sum_{m-\frac{1}{2} < |\mathbf{m}'| \leq m+\frac{1}{2}} P(\mathbf{m}')$. Figure 7 reports the isotropic Hermite spectra $P(m)/P(0)$ (normalized to the mode $m = 0$, which is the only mode excited if the profile is Maxwellian) for the Vlasov and Boltzmann simulations, at both $t = t^*$ and $t = t_{fin}$. As expected, in the collisionless case, a power-law behavior is recovered for a decade of Hermite coefficients (Schekochihin et al. 2008; Tatsuno et al. 2009; Kanekar et al. 2015; Parker et al. 2016; Schekochihin et al. 2016; Servidio et al. 2017; Pezzi et al. 2018a). The Hermite spectrum breaks around $m \simeq 25$, where the artificial dissipation of the Eulerian scheme may affect the dynamics. At $t = t^*$, the energy distribution is quite close to the prediction $P(m) \sim m^{-2}$ (orange line in Fig. 7), which corresponds to the case where magnetic fluctuations are dominant in the cascade process (Servidio et al. 2017).

At a later stage of the Vlasov simulation, the spectrum becomes shallower, indicating an accumulation of enstrophy at higher Hermite coefficients, still compatible with the slope m^{-2} . This accumulation resembles the accumulation of energy in ideal flows, as described in the statistical mechanics of complex systems (Kraichnan 1958; Frisch 1995). The enstrophy cascades to finer scales (higher m 's), there accumulates and might flow back to larger m 's, similarly to MHD (Wan et al. 2009) and similar to plasma echo effects (Gould, O'Neil & Malmberg 1967; Malmberg et al. 1968; Schekochihin et al. 2016; Pezzi, Camporeale & Valentini 2016).

In the collisional case, spectra are less developed, suggesting that collisions cancel the finer scale enstrophy. For the first time, we observe the enstrophy dissipation range in plasma turbulence by using a Boltzmann-like simulation. This is similar to the classical dissipation in Navier-Stokes, where

the dissipative term ($\propto \nabla^2 \mathbf{u}$) suppresses irreversibly the turbulent energy. This suggests that, due to collisions, a significant part of the dynamics in velocity space is forbidden. Note that, according to Pezzi et al. (2018b), the introduction of a collisional operator breaks the enstrophy conservation, which is at the basis of the theory developed in Servidio et al. (2017). It is worth noting, however, that –with respect the classical dissipation in hydrodynamics– the collisional terms are more non-local and their combined effect in physical and velocity space can be much more complex (Pezzi et al. 2018b). As it can be seen from the Hermite spectra, the action of dissipation is already present at m smaller than 10. This might be due to the nonlinear structure of the Dougherty operator, or to the value of ν .

As a byproduct, we can also briefly explain the similar behavior of the entropy density s reported in Fig. 6 for the HVM and HBM cases. Indeed, since Hermite spectra show a power-law behavior, we can expect that the summation in Eq. (10) is dominated by lower Hermite coefficients, where spectra recovered for the collisionless and collisional cases are quite similar; this implying the similar patterns of s reported in Fig. 6.

7. CONCLUSIONS AND DISCUSSIONS

We have investigated the role of proton-proton collisions on the dynamics of weakly-collisional turbulent plasmas by means of direct numerical simulations, where the presence of proton-proton collisions has been modeled through the Dougherty operator. A more complete model, that also takes into account electron dynamics and electron-electron and electron-proton collisions, may partially provide different results, since energy transfers between different species would be allowed. However, because of numerical challenges, it is not possible to address such problem at the present stage.

By comparing the results of collisionless (Vlasov) and collisional (Boltzmann) simulations, we have found that the statistical properties of plasma turbulence at proton inertial scales do not seem to be influenced by inter-particle collisions. On the other hand, the development of kinetic features is strongly suppressed by the presence of collisions, that dissipate non-Maxwellian features, driving plasma towards thermal equilibrium. The temporal range analyzed in the simulation is not long enough to allow collisions to effectively lead the system to equilibrium. However, the temporal evolution of the non-Maxwellian parameter ϵ suggests that, in the presence of collisions, the system will eventually thermalize for times much longer than t_{fin} . It is likely that at such later stage, collisions may also affect the features of turbulence.

Although the presence of collisions strongly attenuate the deviations from the thermodynamic equilibrium, we found that they do not affect the temperature anisotropy. This supports the idea that collisions dissipate different kinetic features on different characteristic time scales. In particular, the dissipation is much faster (i.e. collisionality is locally enhanced) for those phase-space structures that cannot be described in terms of pressure tensor anisotropy (Chew, Goldberger & Low 1956), i.e. the ones associated with fine velocity-space structures (Pezzi, Valentini & Veltri 2016).

The behavior of the collisional dissipation rate (Banón Navarro et al. 2016) and the entropy density (Parks et al. 2012), largely adopted to describe the role of collisions in turbulent plasmas, has been also investigated. Although the collisional dissipation rate adopted does not explicitly include the presence of fine velocity space structures (i.e. is not local in velocity space), it gives important insight on how fast collisions act in a local spatial point, i.e. on the region where heating likely occurs. These regions are well correlated with intense current regions, confirming that plasma heating is an

inhomogeneous process (Osman et al. 2011, 2012; Servidio et al. 2012). The collisional dissipation rate may likely be computed for *in-situ* observations and this will be the content of a future work.

Finally, we found that collisions act in the phase-space cascade, dissipating enstrophy at the finest scales (this increasing plasma entropy), similarly to Navier-Stokes turbulence. As for the termination of the cascade in classical fluids, where energy is cancelled by viscous terms at small spatial scales, here we observe that the collisional operator acts at large values of m , damping the enstrophy cascade (Schekochihin et al. 2016; Eyink 2018).

Estimating similarities and differences between collisional and collisionless dynamics is of fundamental interest for many complex systems. Dissipation in classical fluids is the transfer of macroscopically organized energy to molecular thermal energy. The comparison between simulations of the ideal Euler equations and the dissipative Navier-Stokes model has been an outstanding challenge in the past decades (Morf et al. 1980; Frisch et al. 2008), known as the global regularity problem for the Navier-Stokes equation, and listed in the Clay-Millennium Prize list problems. This problem is intimately related to the question as whether real flows may develop singularities at a finite time. In weakly-collisional plasmas, an equivalent problem could be of fundamental relevance for the Boltzmann-Maxwell system, which ideal counterpart is represented by the Vlasov-Maxwell model. Indeed, the role of collisions in space plasma has been usually interpreted as a secondary effect, due to the small typical collisional coefficients ν . However, just as even very small viscosity plays a crucial role in hydrodynamic turbulence, collisions could be fundamentally important in plasma turbulence. Like in the case of neutral fluids, where $\nabla^2 \mathbf{u}$ can locally become extraordinary intense, the integral in Eq. (6) can become intermittently large, and the associated enstrophy dissipation may become an important ingredient of the cascade. Such interesting analogy should motivate further investigation.

OP sincerely thanks A. Retinò and W. H. Matthaeus for the fruitful discussions. OP and SS are partly supported by the International Space Science Institute (ISSI) in the framework of the International Team 405 entitled “Current Sheets, Turbulence, Structures and Particle Acceleration in the Heliosphere”. DP was supported by STFC grant ST/N000692/1. Numerical simulations discussed here have been performed on the Marconi cluster at CINECA (Italy), within the projects IsC53_RoC-SWT and IsC63_RoC-SWTB, and on the Newton cluster at the University of Calabria (Italy). This project has received funding from the European Unions Horizon 2020 research and innovation programme under grant agreement No 776262 (AIDA).

REFERENCES

Alexandrova, O., Carbone, V., Veltri, P., & Sorriso-Valvo, L. 2008, *Astrophys. J.*, 674, 1153–1157

Anderson, M.W., & O’Neil, T.M. 2007(a), *Phys. Plasmas*, 14, 052103

Anderson, M.W., & O’Neil, T.M. 2007(b), *Phys. Plasmas*, 14, 112110

Bale, S.D., Kellogg, P.J., Mozer, F.S., Horbury, T.S., & Reme, H. 2005, *Phys. Rev. Lett.*, 94, 215002

Balescu R. 1960, *Phys. Fluids* 3, 52

Banón Navarro, A., Teaca, B., Told, D., Groselj, D., Crandall, D., & Jenko, F. 2016, *Phys. Rev. Lett.* 117, 245101.

Bruno, R., & Carbone, V. 2013, *Living Reviews Solar Physics*, 10, 1

Bruno, R., & Telloni, D. 2015, *Astrophys. J. Lett.*, 811, L17

Carbone, F., Sorriso-Valvo, L., Alberti, T., Lepreti, F., Chen, C.H.K., Němeček, Z., & Šafránková, J. 2018, *Astrophys. J.*, 859, 27

Cerri, S.S., Servidio, S., & Califano, F. 2017, *Astrophys. J. Lett.*, 846, L18

Cerri, S.S., Kunz, M.W., & Califano, F. 2018, *Astrophys. J. Lett.*, 856, L13

Chandran, B.D.G. 2010, *Astrophys. J.*, 720, 548–554

Chasapis, A., Yang, Y., Matthaeus, W.H., Parashar, T.N., Haggerty, C.C., Burch, J.L., ..., & Russell, C.T. 2018, *Astrophys. J.*, 862, 32

Chen, C.H.K. 2016, *J. Plasma Phys.*, 82, 53582060

Chen, C.H.K., Matteini, L., Schekochihin, A.A., Stevens, M.L., Salem, C.S., Maruca, B.A., Kunz, M.W., & Bale S.D. 2016, *Astrophys. J. Lett.*, 825, L26

Chew, G. F., Goldberger, M. L., & Low, F. E. 1956, *Proc. R. Soc. Lond. A*, 236, 112–118

Chhiber, R., Usmanov, A. V., Matthaeus, W. H., & Goldstein, M. L. 2016, *Astrophys. J.*, 821, 34

Dae Yoon, Y., & Bellan, P.M. 2018, *Astrophys. J. Lett.*, 868, L31

Dougherty, J.P. 1964, *Phys. Fluids*, 7, 1788

Dougherty, J.P., & Watson, S.R. 1967, *J. Plasma Phys.*, 1, 317–326

Dougherty, J.P., Watson, S.R., & Hellberg, M.A. 1967, *J. Plasma Phys.*, 1, 327–339

Escande, D., Elskens, Y., & Doveil, F. 2015, *J. Plasma Phys.*, 81, 305810101
doi:10.1017/S0022377814000415

Eyink, G.L. 2018, *Phys. Rev. X*, 8, 041020

Filbet, F., & Pareschi, L. 2002, *J. Comput. Phys.*, 179, 1

Franci, L., Landi, S., Verdini, A., Matteini, L., & Hellinger, P. 2018, *Astrophys. J.*, 853, 26

Frisch, U. 1995, *Turbulence: the legacy of A.N. Kolmogorov* (Cambridge university press, Cambridge).

Frisch, U., Kurien, S., Pandit, R., Pauls, W., Ray, S.S., Wirth, A., & Zhu, J.Z. 2008, *Phys. Rev. Lett.*, 101, 144501

Gary, S.P. 2005, *Theory of space plasma microinstabilities*, (Cambridge university press, Cambridge).

Gary, S. P., Zhao, Y., Hughes, R. S., Wang, J., & Parashar, T. N. 2018, *Astrophys. J.*, 859, 110

Gould, R., O’Neil, T.M., & Malmberg, J.H. 1956, *Phys. Rev. Lett.*, 19, 219

Greco, A., Valentini, F., Servidio, S., & Matthaeus, W.H. 2012, *Phys. Rev. E*, 86, 066405

Greco, A., Perri, S., Servidio, S., Yordanova, E., & Veltri, P. 2016, *Astrophys. J. Lett.*, 823, L39

Groselj, D., Cerri, S.S., Navarro, A.B., Willmott, C., Told, D., Loureiro, N.L., Califano, F., & Jenko, F. 2017, *Astrophys. J.*, 847, 28

Hellinger, P., Landi, S., Matteini, L., Verdini, A., & Franci, L. 2017, *Astrophys. J.*, 838, 158

Hellinger, P., Verdini, A., Landi, S., Franci, L., & Matteini, L. 2018, *Astrophys. J. Lett.*, 857, L19

Hernandez, R., & Marsch, E. 1985, *J. Geophys. Res.*, 90, 11062

Kanekar, A., Schekochihin, A.A., Dorland, W., & Loureiro, N.F. 2015, *J. Plasma Phys.*, 81, 305810104

Karimabadi, H., Roytershteyn, V., Wan, M., Matthaeus, W.H., Daughton, W., Wu, P., Shay, M., Loring, B., Borovsky, J., Leonardis, E., Chapman, S.C., & Nakamura, T.K.M. 2013, *Phys. Plasmas*, 20, 012303

Karimabadi, H., Roytershteyn, V., Daughton, W., & Liu, Y. 2013, *Space Sc. Rev.*, 178, 307

Kasper, J.C., Lazarus, A.J., & Gary, S.P. 2008, *Phys. Rev. Lett.* 101, 261103

Kolmogorov, A. N., 1941, *Dokl. Akad. Nauk. SSSR* 30, 301

Kraichnan, R.H. 1958, *Phys. Rev.*, 109(5), 1407

Landau, L.D. 1936, *Phys. Z. Sovjet*, 154, translated in *Collected papers of L.D. Landau* edited by D. ter Haar pp 163–170 (Oxford: Pergamon, 1981).

Lapenta, G., Berchem, J., Zhou, M., Walker, R.J., El-Alaoui, M., Goldstein, M.L., ..., & Burch, J.L. 2017, *J. Geophys. Res. Space Physics*, 122, 2024–2039

Leamon, R. J., Smith, C. W., Ness, N. F., matthaeus, W. H., and Wong, H. K. 1998, *J. Geophys. Res.* 103, 4775

Lenard, A. 1960, *Ann. Phys.*, 10, 390

Liang, H., Cassak, P.A., Servidio, S., Shay, M.A., Drake, J.F., Swisdak, M.S., ..., & Delzanno G.L. 2019, arXiv:1902.02733

Li, T.C., Howes, G.G., Klein, K.G., & TenBarge, J.M. 2016, *Astrophys. J. Lett.*, 832, L24

Livi, S., Marsch, E., & Rosenbauer, H. 1986, *JGRA*, 91, 8045

Malmberg, J.H., Wharton, C.B., Gould, R.W. & O’Neil, T.M. 1968, *Phys. Rev. Lett.*, 20, 95

Marino, R., Sorriso-Valvo, L., Carbone, V., Noullez, A., Bruno, R., & Bavassano, B. 2008, *Astrophys. J.*, 677, L71–L74

Marsch, E. 2006, *Living Rev. Sol. Phys.*, 3, 1

Maruca, B.A., Kasper, J.C., & Bale, S.D. 2011, *Phys. Rev. Lett.*, 107, 201101

Maruca, B.A., Bale, S.D., Sorriso-Valvo, L., Kasper, J.C., & Stevens, M.L. 2013, *Phys. Rev. Lett.*, 111, 241101

Matteini, L., Hellinger, P., Landi, S., Travnicek, P., & Velli, M. 2012, *Space Sci. Rev.*, 172, 373–396 DOI 10.1007/s11214-011-9774-z

Morf R.H., Orszag S.A., & Frisch U. 1980, *Phys. Rev. Lett.*, 44, 572

Osman, K.T., Matthaeus, W.H., Greco, A., & Servidio, S. 2011, *Astrophys. J. Lett.*, 727, L11

Osman, K.T., Matthaeus, W.H., Wan, M., & Rappazzo, A.F. 2012, *Phys. Rev. Lett.*, 108, 261102

Parizot, E., Marcowith, A., Ballet, J., & Gallant, Y.A., 2006, *Astron. & Astrophys.*, 453, 387–395

Parker, J.T., Highcock, E.G., Schekochihin, A.A., & Dellar, P.J. 2016, *Phys. Plasmas*, 23, 070703

Parks, G. K., Lee, E., McCarthy, M., Goldstein, M., Fu, S. Y., Cao, J. B., ... & Réme, H. 2012, *Phys. Rev. Lett.*, 108, 061102

Perri, S., Goldstein, M.L., Dorelli, J.C., & Sahraoui, F. 2012, *Phys. Rev. Lett.*, 109, 191101

Perrone, D., Valentini, F., Servidio, S., Dalena, S., & Veltri, P. 2013, *Astrophys. J.*, 762, 99

Perrone, D., Alexandrova, O., Mangeney, A., Maksimovic, M., Lacombe, C., Rakoto, V., Kasper, J.C., & Jovanovic, D. 2016, *Astrophys. J.*, 826, 166

Perrone, D., Alexandrova, O., Roberts, O. W., Lion, S., Lacombe, C., Walsh, A., ... & Zouganelis, I. 2017, *Astrophys. J.*, 849(1), 49

Perrone, D., Passot, T., Laveder, D., Valentini, F., Sulem, P.L., Zouganelis, I., Veltri, P., & Servidio, S. 2018, *Phys. Plasmas*, 25, 052302

Pezzi, O., Valentini, F., Perrone, D., & Veltri, P. 2013, *Phys. Plasmas*, 20, 092111; *Phys. Plasmas*, 21, 019901

Pezzi, O., Valentini, F., & Veltri, P. 2015a, *J. Plasma Phys.*, 81(1), 305810107

Pezzi O., Valentini F., & Veltri, P. 2015b, *Phys. Plasmas*, 22(4), 042112

Pezzi, O., Valentini, F., & Veltri, P. 2016, *Phys. Rev. Lett.*, 116, 145001

Pezzi, O., Camporeale, E., & Valentini, F. 2016, *Phys. Plasmas*, 23, 022103

Pezzi, O. 2017, *J. Plasma Phys.*, 83, 555830301

Pezzi, O., Parashar, T.N., Servidio, S., Valentini, F., Vásconez, C.V., Yang, Y., Malara, F., Matthaeus, W.H., & Veltri, P. 2017, *Astrophys. J.*, 834, 166

Pezzi, O., Parashar, T.N., Servidio, S., Valentini, F., Vásconez, C.V., Yang, Y., Malara, F., Matthaeus, W.H., & Veltri, P. 2017, *J. Plasma Phys.*, 83, 905830105

Pezzi, O., Servidio, S., Perrone, D., Valentini, F., Sorriso-Valvo, L., Greco, A., Matthaeus, W.H., & Veltri, P. 2018a, *Phys. Plasmas*, 25, 060704

Pezzi, O., Valentini, F., Servidio, S., Camporeale, E., & P., Veltri, *Fourier-Hermite decomposition of the collisional Vlasov-Maxwell system: implications for the velocity space cascade*, 2018b submitted to *Plasma Phys. Control. Fus.*

Rosenbluth, M.N., MacDonald, W.M., & Judd, D.L. 1957, *Phys. Review*, 107, 1

Sahraoui, F., Goldstein, M.L., Robert, P., & Khotyaintsev, Yu.V. 2009, *Phys. Rev. Lett.*, 102, 231102 & Belmont, G. 2007, *J. Plasma Phys.*, 73, 723

Schekochihin, A.A., Cowley, S.C., Dorland, W., Hammett, G.W., Howes, G.G., Plunk, G.G., Quataert, E., & Tatsuno, T. 2008, *Plasma Phys. Control. Fusion*, 50, 124024

Schekochihin, A.A., Parker, J.T., Highcock, E.G., Dellar, P.J., Dorland, W., & Hammett, G.W. 2016, *J. Plasma Phys.*, 82, 905820212

Servidio, S., Valentini, F., Califano, F., & Veltri, P. 2012, *Phys. Rev. Lett.*, 108, 045001

Servidio, S., Valentini, F., Perrone, D., Greco, A., Califano, F., Matthaeus W.H., & Veltri, P. 2015, *J. Plasma Phys.*, 81, 325810107

Servidio, S., Chasapis, A., Matthaeus, W.H., Perrone, D., Valentini, F., Parashar, T.N., ... & Burch, J. 2017, *Phys. Rev. Lett.*, 119, 205101

Shay, M.A., Haggerty, C.C., Matthaeus, W.H., Parashar, T.N., Wan, M., & Wu, P. 2018, *Phys. Plasmas*, 25, 012304

Spitzer, L. Jr. 1956 *Physics of Fully Ionized Gases*, Interscience Publishers

Sorriso-Valvo, L., Carbone, V., Veltri, P., Consolini, G., & Bruno, R. 1999, *Geophys. Res. Lett.*, 26, 1801–1804

Sorriso-Valvo, L., Marino, R., Carbone, V., Noullez, A., Lepreti, F., Veltri, P., ... & Pietropaolo, E. 2007, *Phys. Rev. Lett.*, 99, 115001

Sorriso-Valvo, L., Catapano, F., Retin, A., Le Contel, O., Perrone, D., Roberts, O. W., ... & Khotyaintsev, Yu.V., 2019, *Phys. Rev. Lett.*, 122(3), 035102

Tatsuno, T., Dorland, W., Schekochihin, A.A., Plunk, G.G., Barnes, M., Cowley, S.C., & Howes, G.G. 2009, *Phys. Rev. Lett.*, 103, 015003

TenBarge, J.M., & Howes, G.G. 2013, *Astrophys. J. Lett.*, 771, L27

Tigik, S.F., Ziebell, L.F., Yoon, P.H., & Kontar, E.P. 2016, *Astron. and Astrophys.*, 586, A19

Tracy, P.J., Kasper, J.C., Raines, J.M., Shearer, P., Gilbert, J.A., & Zurbuchen, T.H. 2016, *Phys. Rev. Lett.* 116, 255101

Vafin, S., Riazantseva, & Pohl, M. 2019 *Astrophys. J. Lett.*, 871, L11

Vaivads, A., Retinò, A., Soucek, J., Khotyaintsev, Yu.V., Valentini, F., Escoubet, C.P., ..., & Burgess, D. 2016, *J. Plasma Phys.*, 82, 905820501

Valentini, F., Travnicek, P., Califano, F., Hellinger, P., & Mangeney, A. 2007, *J. Comput. Phys.*, 225, 753

Valentini, F., Servidio, S., Perrone, D., Califano, F., Matthaeus, W. H., & Veltri, P. 2014, *Physics of Plasmas*, 21, 082307

Valentini, F., Perrone, D., Stabile, S., Pezzi, O., Servidio, S., De Marco, R., ... & Veltri, P. 2016, *New J. Phys.*, 18, 125001

Vásconez, C.L., Pucci, F., Valentini, F., Servidio, S., Matthaeus, W.H., & Malara, F. 2015, *Astrophys. J.*, 815, 7

Vech, D., Klein, K.G., & Kasper, J.C. 2017, *Astrophys. J. Lett.*, 850, L11

Veltri, P. 1999, *Plasma Phys. Control. Fus.*, 41, A787 <http://stacks.iop.org/0741-3335/41/i=3A/a=071>

Wan, M., Oughton, S., Servidio, S. & Matthaeus, W.H. 2009, *Phys. Plasmas*, 16, 080703

Wan, M., Matthaeus, W.H., Karimabadi, H., Roytershteyn, V., Shay, M., Wu, P., Daughton, W., Loring, B. & Chapman, S.C. 2012, *Phys. Rev. Lett.*, 109, 195001

Wan, M., Matthaeus, W.H., Roytershteyn, V., Karimabadi, H., Parashar, T., Wu, P., & Shay, M. 2015, *Phys. Rev. Lett.*, 114, 175002

Wang, T., Alexandrova, O., Perrone, D., Dunlop, M., Dong, X., Bingham, R., ... & Ergun, R. E. 2019, *Astrophys. J. Lett.*, 871, L22

Webb, G.M., Barghouty, A.F., Hu, Q., & Le Roux, J.A. 2018, *Astrophys. J.*, 855, 31

Wilder, F.D., Ergun, R.E., Schwartz, S.J., Newman, D.L., Eriksson, S., Stawarz, J.E., ..., & Magnes, W. 2016, *Geophys. Res. Lett.*, 43, 8859–8866, doi:10.1002/2016GL070404.

Wu, P., Perri, S., Osman, K., Wan, M., Matthaeus, W. H., Shay, M. A., ... & Chapman, S. 2013, *Astrophys. J. Lett.*, 763, L30

Yang, Y., Matthaeus, W.H., Parashar, T.N., Haggerty, C.C., Roytershteyn, V., Daughton, W., ..., & Chen, S. 2017, *Phys. Plasmas*, 24, 072306

Yin, Z. 2014, *J. Comput. Phys.*, 258, 371

Zimbardo G., Greco A., Sorriso-Valvo L., Perri S., Voros Z., Aburjania G., Chargazia K., & Alexandrova O. 2010, *Space Sc. Rev.* 156, 89